The Preparation of the Chromized Coatings on AISI 1045 Carbon Steel Plate with the Electroplating Pretreatment of Ni or Ni/Cr-C Film

Lin-Chang Tsai[1], Hung-Hua Sheu[2], Cheng-Chieh Chen[2], Ming-Der Ger[2,]*

[1] Department of Mechatronic, Energy & Aerospace Engineering, Chung Cheng Institute of Technology, National Defense University, Taiwan, ROC
[2] Department of Chemistry & Materials Engineering, Chung Cheng Institute of Technology, National Defense University, Taiwan, ROC
[*]E-mail: mingderger@gmail.com, mdger@ndu.edu.tw

Chromized coatings on AISI 1045 steel were prepared as bipolar plates for proton exchange membrane fuel cells (PEMFCs) by low-temperature pack chromization. Before pack chromization, two kinds of pretreatment processes including the Ni electroplating and the Ni electroplating, followed by Cr-C electroplating were used to activate the steel surface. The additional Cr-C electroplating promotes the chromization rate, resulting in a thicker chromized coating (1045-Ni-CrC-Cr(700-2)) with higher carbides and nitrides contents. The 1045-Ni-CrC-Cr(700-2) specimen shows the lowest corrosion current density, 8.37×10^{-8} Acm^{-2}, and the smallest interfacial contact resistance, 14 mΩ-cm^2, at 140 Ncm^{-2} among all tested steels. The 1045-Ni-CrC-Cr(700-2) specimen also had high surface energy. The contact angle of the 1045-Ni-CrC-Cr(700-2) with water was about 100˚, which is beneficial for water management in a fuel cell. This study clearly indicates that the additional Cr-C electroplating pretreatment step can improve the properties of chromized 1045 steel tremendously, which possess the potential to be bipolar plates in the application of PEMFC.

1. INTRODUCTION

The proton exchange membrane fuel cells (PEMFC) are expected to be a potentiality energy device due to its noisy-free, low operating temperature, high-energy efficiency, high-reliability and low-emission. Bipolar plates constitute the backbone of a PEMFC power stack, conduct current between cells, facilitate water and thermal management through the cell, and provide conduits for

reactant gases namely hydrogen and oxygen. Accordingly, bipolar plates must be electrically conducting, mechanically and chemically stable, made of low permeability materials, corrosion resistant, allow uniform reactant gas distribution and product removal, and easy manufactured for cost effectiveness. Due to metallic bipolar plats for the PEMFC offer many advantages, including easy manufacturing, excellent mechanical properties, high volumetric power density and relatively low cost, bipolar plates based on metals have recently attracted the attention of the scientific community [1]. Various metals such as titanium, aluminum, and stainless steel have been studied as alternative bipolar plate materials for PEMFCs [2-8].

Among the available metals, stainless steel has been considered as a potential candidate because of its suitable physical and mechanical properties with relatively low prices. However, metal bipolar plates are exposed to an acidic (pH 2-3) and humid environment at temperatures of around $80^{o}C$, and are prone to corrosion or dissolution in a PEMFC system. The dissolved metal ions may poison membrane electrode assembly and decline the performance of fuel cells [9,10]. Additionally, oxidation of metal occurs in the operating environment of PEMFCs, resulting in an increase of the interfacial contact resistance between bipolar plates and gas diffusion layers, and a reduction of the fuel cell efficiency. Protecting metal bipolar plates from the corrosive fuel cell operating conditions with coatings is generally used to increase the corrosion resistance and decrease the contact resistance [11-22].

Pack chromization is one of the easiest and cheapest processes to obtain the chromizing coatings to improve the corrosion resistance, hardness, and weariness of various carbon steels [23, 24]. Unfortunately, the pack cementation was normally performed at temperatures above $1000^{o}C$ for durations of about 6 - 10 h. Such a high temperature treatment inevitably limits the applications of chromizing coatings due to grain growth of the substrate materials, which has a detrimental effect on the mechanical properties of work pieces. Therefore, reducing pack-cementation temperature is required for widespread application of the chromizing coatings. Generally, the operation temperature can be decreased by activating the surface of the base metal [25]. In our previous study [26], we have found that the corrosion resistance and superficial conductivity of 1020 carbon steel can be enhanced significantly by the pretreatments of nickel electroplating combined with low-temperature pack chromization. However, the nickel layer can not totally block the Fe diffusing from matrix to surface during the chromizing process. The Fe element existed in the surface of chromized coating is detrimental to the corrosion resistance of the chromized coating. On the other hand, it has been reported that the performances of chromized coatings are somewhat dependent on the amount of carbon in substrates. Steels contain the higher carbon concentration, the larger qualities of chromium carbides were produced in chromized coatings leading to better properties [27]. It suggests that producing a Cr-C coating on the metal substrates not only might act as an additional barrier to block the Fe diffusing out but also can offer the driving force to promote the chromization rates.

To enhance the corrosion resistance and electrical conductivity of metal bipolar plates by low-temperature pack cementation, a two-step electroplating pretreatment was designed in the present work. The first step was to electroplate a nickel inner layer, and the second step was to electroplate a Cr-C layer onto the nickel inner layer. The deposition behaviors and characteristics of these AISI 1045

steels with chromized coatings were investigated. Similar chromization was also carried out on the AISI 1045 steel pretreated with Ni electroplating only for comparison.

2. EXPERIMENTAL

2.1 Pack cementation on AISI 1045 carbon steel sheet

The AISI 1045 carbon steel sheet was used as the substrate in this experiment. The composition of the AISI 1045 carbon steel is shown in Table 1.

Table 1. Chemical composition of AISI 1045 carbon steel.

Elements	C	Cu	Mn	P	Fe
wt(%)	0.4-0.5	<0.25	<0.7	<0.01	Balance

The sheet was cut into 30 mm×30 mm×3 mm plates for the surface pretreatment and subsequent pack cementation. Before the surface pretreatment, the AISI 1045 steel sheets were polished with silicon carbide abrasive papers from #100 to #800 and were degreased with acetone using an ultrasonic cleaner, blow-dried with nitrogen gas, and then kept in a vacuum pot to avoid producing oxide layer and rust spots and to make uniform surface condition.

Before pack cementation, substrate was pretreated by Ni electroplating or a combination of Ni electroplating and Cr-C electroplating to activate the surface. The Ni layer was deposited from an electrolyte containing 400 gl^{-1} Ni(NH$_2$SO$_3$)$_2$ and 30 gl^{-1} H$_3$BO$_3$ using the DC plating technique at current density of 2.5 Adm^{-2} (ASD), room temperature and pH=4 for 20 min. The composition of trivalent chromium plating bath for this study was: 106 gl^{-1} CrCl$_3$ as a source of Cr^{+3}, 133 gl^{-1} NH$_4$Cl as conductive salt, 15 gl^{-1} NH$_4$Br as antioxidizing agent, 54 gl^{-1} acetic acid (CH$_3$COOH) as complexing agent and 40 gl^{-1} H$_3$BO$_3$ as buffer. The Cr-C electroplating was carried out for 5 min with the conditions of 10 ASD, room temperature, and pH of 3.0.

The pack chromization process was used to deposit the chromized coatings on the pretreated specimens. Chromizing on the samples pretreated with the electroplated Ni layer and Ni/Cr-C layer was carried out using pack cementation at 700°C for 2 h in a homogeneous mixture of 15 wt.% Cr powder as master alloy source, 10 wt.% NH$_4$Cl as activator and 75 wt.% Al$_2$O$_3$ as inert filler in an Ar atmosphere. The powder mixture was mixed up and homogenized using ball mill for 12 h. Specimens were buried in the pack powders filled in a cylindrical alumina crucible. The crucible was placed in a chamber and then vacuumed at an environment of 10^{-3} Torr to prevent specimens from oxidation. The pack was heated from room temperature to 150 ^{o}C at a rate of 10°C min^{-1} and then held at the temperature for 1 h, then enhanced the temperature to 700°C and held for 2 h. Various chromized coatings have been simply named, and the specimen names and corresponding conditions are shown as Table 2.

Table 2. Code-name list of specimens

Code-name of specimen	Pretreatment	Chromization temp. and duration
1045	-	-
1045-Ni	Ni	-
1045-Ni-CrC	Ni-CrC	-
1045-Ni-Cr(700-2)	Ni	700˚C, 2hr
1045-Ni-CrC-Cr(700-2)	Ni-CrC	700˚C, 2hr

2.2 Characterization of chromizing coatings

Scanning electron microscope (SEM) was employed to analyze the microstructure and morphology of the coatings. The crystalline structures and constituent phases of the coatings were examined by X-ray diffraction (XRD) with Cu Kα radiation ($\lambda = 0.15405$ nm) over a scanning range from 20˚ to 80˚. The distribution of Fe, C, Ni, Cr and N in the coatings was assessed with an electron probe X-ray micro-analyzer (EPMA).

The deposition rate of the chromizing coatings was estimated by measuring the weight before and after cementation process using an electrical balance with 0.01 mg weight scale accuracy.

Potentiodynamic polarization tests were carried out in a three-electrode cell system in which a platinum sheet and an Ag/AgCl electrode (197 mV vs. SHE) were used as the counter and reference electrodes, respectively. The working electrode was a bare AISI 1045 steel plate, Ni coated AISI 1045 steel plate, Ni/CrC coated AISI 1045 steel plate, or the chromized AISI 1045 steel plate. Geometric area of the tested specimens is 1 cm^2 in the corrosion experiments. The corrosion behavior of all samples was tested in a 0.5 M H_2SO_4 aqueous solution at room temperature. All experiments were performed using an Autolab PGSTAT30 potentiostat/galvanostat controlled by the GPES (General Purpose Electrochemical System) software. The linear polarization curves were measured in the potential range between -0.3 V and 0.8 V, with a scanning rate of 0.5 mVs^{-1}. Before the tests, all specimens were degreased and rinsed with deionized water. A fresh corrosion bath was used for each new specimen. When potentiostatic tests were performed, the 0.6 V (vs. SCE) potential with air purging was applied to simulate the cathodic environment in a 0.5M H_2SO_4 solution at 80°C for 1 h.

Interfacial contact resistance (ICR) under various compaction forces were measured following the method described in Ref. [27]. For measuring the contact resistance, two pieces of carbon paper were sandwiched between the specimen and two copper plates. During the tests, a constant electrical current was provided through the copper plates, and the variation in the total voltage was recorded with respect to the compaction force that was steadily increased from 0 to 200 Ncm^{-2} and recorded with every 9.8 Ncm^{-2}.

Contact angle of the bipolar plate sample with water was measured by a contact angle goniometer (FACE CA-5 150, Tantec, USA) under room temperature to investigate the surface energy. All measurements of contact angle were repeated five times on other places of the same specimen. The reported value for each sample is the mean of five measurements.

3. RESULTS AND DISCUSSION

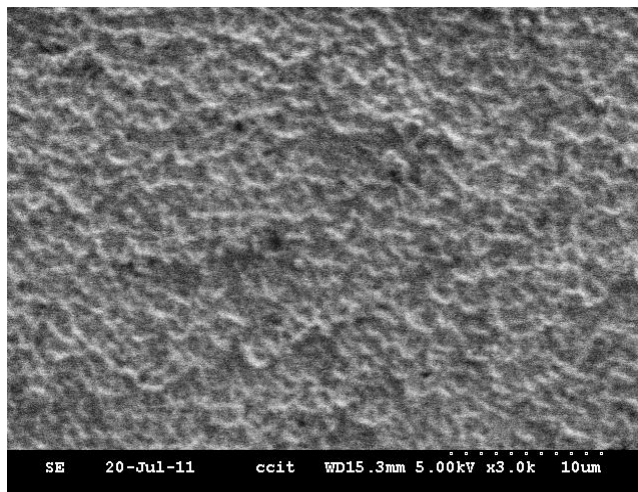*3.1 Surface and cross-sectional morphology*

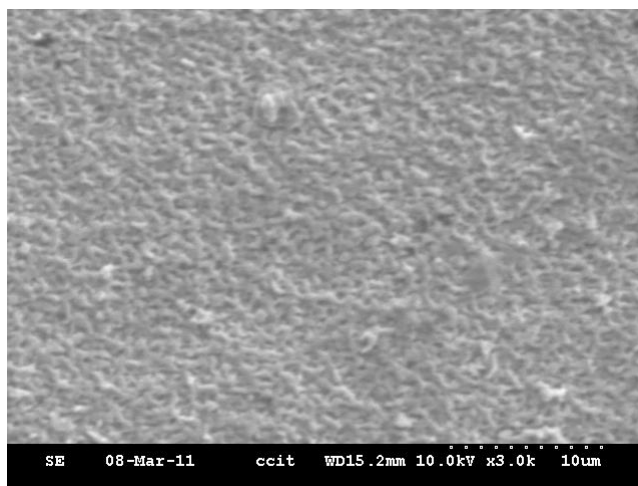**Figure 1.** SEM micrograph of the surface of the 1045-Ni-Cr(700-2).

Figure 2. SEM micrograph of the surface of the 1045-Ni-CrC-Cr(700-2).

Surface morphologies of specimen 1045-Ni-Cr(700-2) and 1045-Ni-CrC-Cr(700-2) chromized at 700°C for 2 h are shown in Fig. 1. It shows from Fig. 1 that a flat and continuous chromized layer was deposited on both AISI 1045 steels with different pretreatment conditions. Surface morphology of sample 1045-Ni-CrC-Cr(700-2) is a little denser and smoother than that of sample 1045-Ni-Cr(700-2), which should be due to the presence of an additional Cr-C layer on the surface before pack chromization was performed. The cross-section morphologies of these chromized coatings are shown in Fig. 2. It is clear that a continuous chromized layer is deposited on the substrate. Cr-enriched layer about 3.5 μm is formed in sample 1045-Ni-CrC-Cr(700-2), which is thicker than that of sample 1045-Ni-Cr(700-2) (about 1.5-2.0 μm). Due to its difficulty to distinguish the electroplated Cr-C layer and chromized layer, the exact thickness of chromized layer in sample 1045-Ni-CrC-Cr(700-2) is

unknown. Thus, to examine the effect of electroplated Cr-C layer on the chromization, the weight change after each step was measured and listed in Table 3.

Table 3. Weight variation after each step during fabrication of chromized coatings.

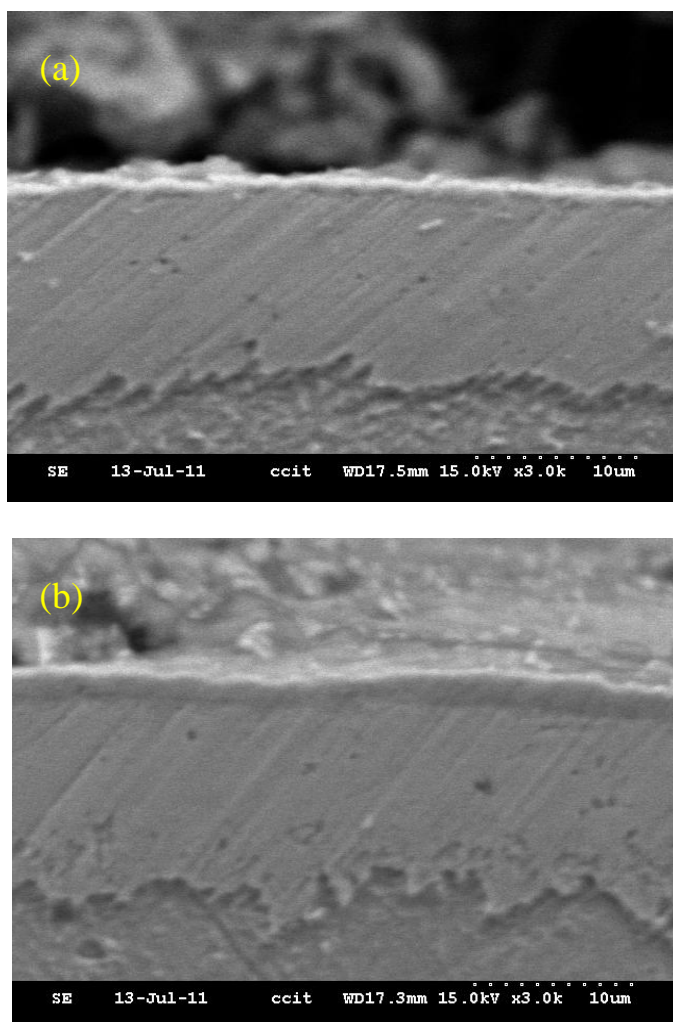| Code-name of specimen	Weight difference after nickel electrodeposited	Weight difference after Cr-C electrodeposited	Weight difference after chromized by pack cementation	Weight increase after pack cementation
1045-Ni-Cr(700-2)	13.50337 g	-	13.50648 g	+0.00311 g
1045-Ni-CrC-Cr(700-2)	13.65111 g	13.65131 g	13.65597 g	+0.00466 g

Figure 3. The cross-sectional SEM image of (a)1045-Ni-Cr(700-2), and (b)1045-Ni-CrC-Cr(700-2).

As can be clearly seen from Table 3, the weight increase after pack cementation for sample 1045-Ni-CrC-Cr(700-2) (0.00466 g) is about 1.5 time higher than that of sample 1045-Ni-Cr(700-2)

(0.00311 g), suggesting the chromized layer in sample 1045-Ni-CrC-Cr(700-2) should be thicker than that of sample 1045-Ni-Cr(700-2).
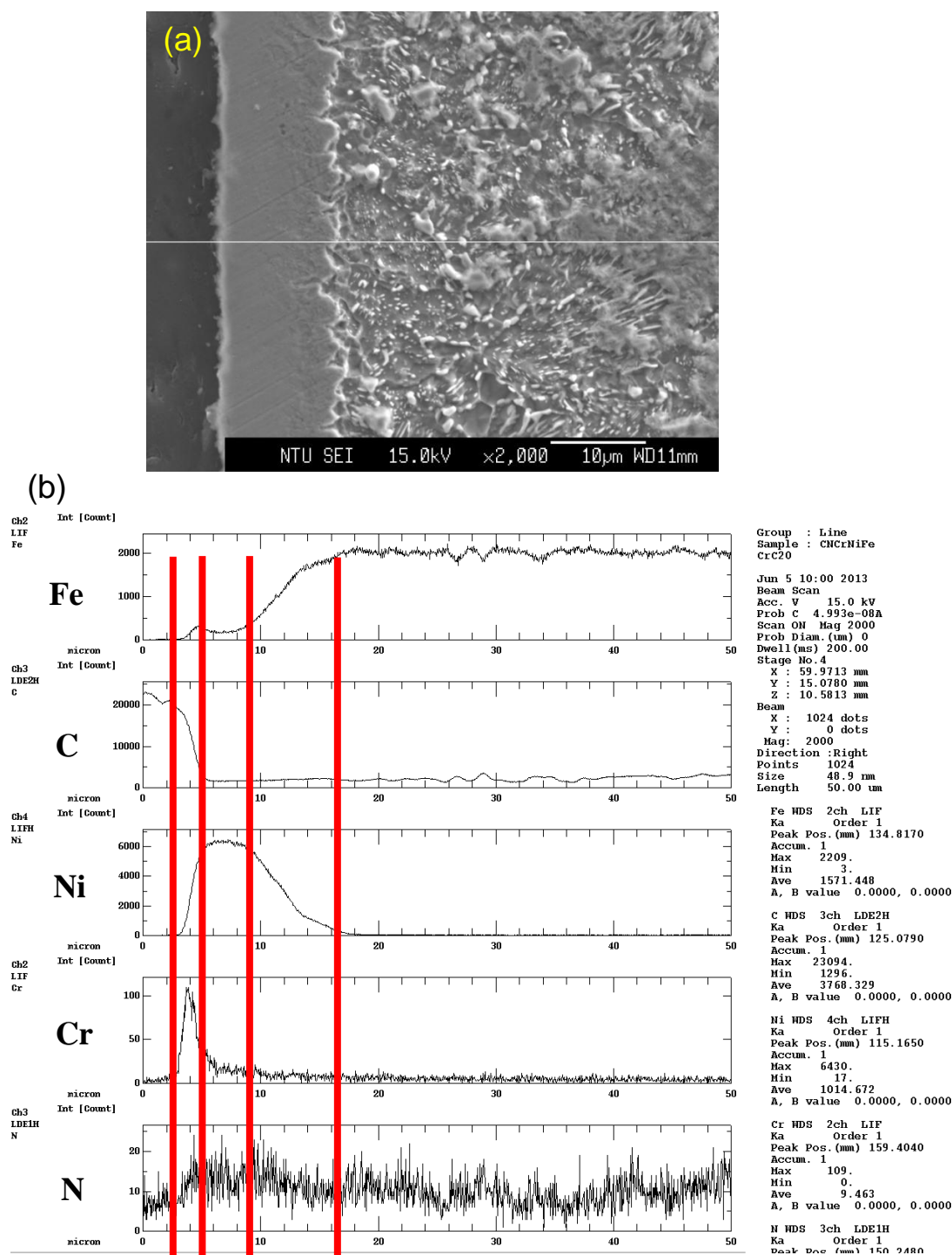

Figure 4. (a) The Cross-sectional SEM micrograph of 1045-Ni-CrC-Cr(700-2) followed by (b) EPMA line-scan of Fe, C, Ni, Cr and N in (a).

Therefore, a combination of nickel electroplating and Cr-C electroplating pretreatments can produce a chromized coating thicker than that of simple activating treatment by nickel electroplating

on substrate due to the additional activating treatment by Cr-C electroplating increases the carbon content on the substrate surface which hastening the deposition rate of chromium. Lee et al. reported a similar trend on the chromized steels with different carbon contents [28].

Fig. 4 is cross-sectional SEM micrographs with elemental line scan of sample 1045-Ni-CrC-Cr(700-2). A double layer structure was observed obviously in the cross-section morphologies (Fig. 4(a)), the outermost is a chromium-riched layer, followed by nickel-iron solid solution and/or intermetallics layer. It shows from Fig. 4(b) that the concentration of chromium was highest at the near-surface region in the nickel layer, which is consistent with our previous study on chromized 1020 steel with Ni electroplating pretreatment [26]. Fig. 4(b) also reveals that the carbon concentration is the highest near the free surface and gradually decreases until the abrupt drop at the boundary between the Cr-rich layer and the nickel layer and only a little concentration of Fe element exists in the outer coating. In general, the chromized coatings on Fe-based steels are consisted mainly of chromium carbides, chromium nitrides, and a small amount of metal oxides [29]. The result indicates that chromized coating contains a significant amount of Cr-carbide and a little amount of Cr-nitride distributing near the surface of coating for specimen 1045-Ni-CrC-Cr(700-2). Thus, it is expected that 1045-Ni-CrC-Cr(700-2) coating possess excellent corrosion resistance. The Ni-Fe solid solution and Ni-Fe alloy inner layer was formed in the depth range of $9 - 16$ μm beneath surface, which can be attributed to nickel and iron atoms have a high miscibility in high temperature environment [30].
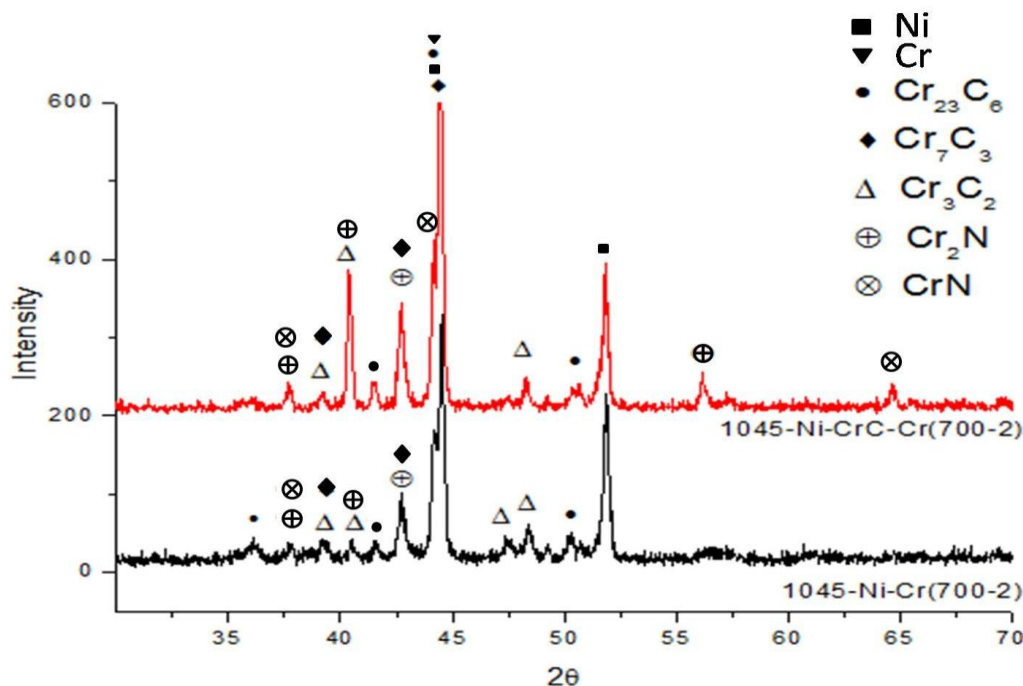
3.2 X-ray diffraction (XRD) analysis

Figure 5. X-ray diffraction patterns of specimens 1045-Ni-Cr(700-2) and 1045-Ni-CrC-Cr(700-2)

Fig. 5 shows the XRD pattern of specimens of 1045-Ni-Cr(700-2) and 1045-Ni-CrC-Cr(700-2), respectively. The X-ray diffraction patterns for specimens with different pretreatments revealed similar results. The coatings are mainly consisted of the mixtures of Ni, Cr, chromium carbides (i.e. $Cr_{23}C_6$, Cr_7C_3, Cr_3C_2) and chromium nitrides (i.e. Cr_2N, CrN), which is in good agreement with the results of line scanning analysis. And, the peaks of chromium carbides and nitrides in sample 1045-Ni-CrC-Cr(700-2) are more intensive than those in sample 1045-Ni- Cr(700-2). The chromium carbides and nitrides existing in the coatings could improve both corrosion resistance and surface conductivity of the modified steels [31-33]. Additionally, the oxides were not formed on the surface of chromized coatings, which might be ascribed to the pack cementation was performed under a protective atmosphere (argon gas).

3.3 Corrosion resistance

Table 4. The polarization characteristics of bare and various coated steels evaluated in the potentiodynamic test.

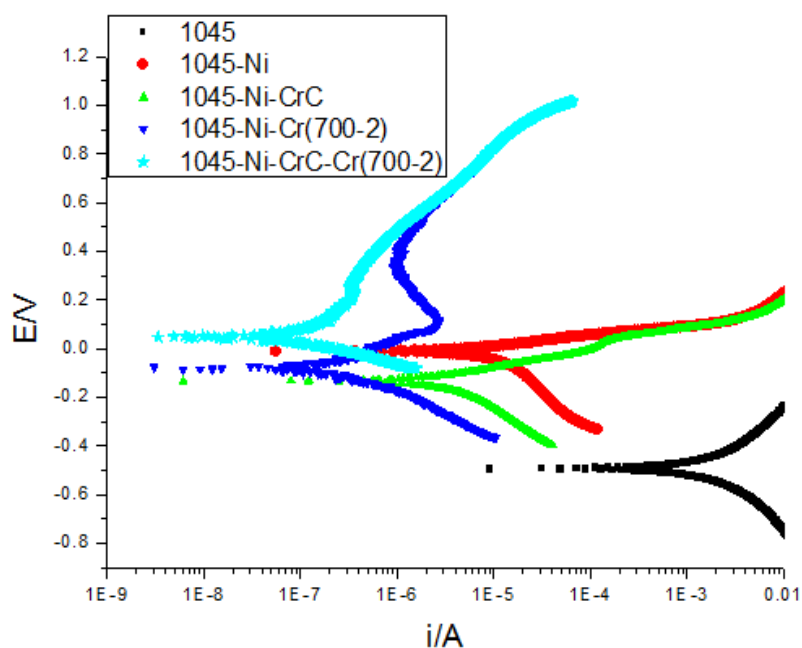| Code-name of specimen	Corrosion potential (E_{corr}) V	Corrosion current (I_{corr}) A/cm^2	Anodic Tafel slope
1045	-0.48	1.61E-3	0.049
1045-Ni	-0.01	8.57E-6	0.040
1045-Ni-CrC	-0.14	2.86E-6	0.062
1045-Ni-Cr(700-2)	-0.08	2.25E-7	0.034
1045-Ni-CrC-Cr(700-2)	0.05	8.37E-8	0.055

Figure 6. Polarization curves of bare and various chromized 1045 steels measured in a 0.5M H_2SO_4 solution at room temperature.

Fig. 6 shows potentiodynamic polarization curves for 1045 steel without and with pretreated and chromized coatings in a 0.5 M H_2SO_4 solution at room temperature. The corrosion current density (I_{corr}) and corrosion potential (E_{corr}) are calculated from the intercept of the Tafel slopes, and are given in Table 4. The uncoated steel shows a corrosion potential of -0.48 V vs SCE and a corrosion current density (I_{corr}) of 1.61×10^{-3} Acm^{-2}. After the electroplating Ni and Ni/Cr-C pretreatments, the I_{corr} of 1045-Ni (8.57×10^{-6} Acm^{-2}) and 1045-Ni-CrC (2.86×10^{-6} Acm^{-2}) are about three order magnitude lower than that for bare 1045 steel. Meanwhile, the corrosion potential E_{corr} of 1045-Ni and 1045-CrC shifts markedly to positive direction by contrast to the untreated 1045 steel. In comparison with the Ni coated and Cr/C coated AISI 1045 steels, the chromized specimens exhibit a lower corrosion current. The corrosion current densities of 1045-Ni-Cr(700-2) and 1045-Ni-CrC-Cr(700-2) are 2.25×10^{-7} and 8.37×10^{-8} Acm^{-2}, respectively. The I_{corr} values of all chromized layer coated samples were lower than the US DOE target of 1×10^{-6} Acm^{-2} [34]. The corrosion current density (I_{corr}) of all tested specimens is in the order of bare steel > 1045-Ni > 1045-Ni-CrC > 1045-Ni-Cr(700-2) > 1045-Ni-CrC-Cr(700-2). In other words, the sample 1045-Ni-CrC-Cr(700-2) exhibits the best corrosion resistance among all tested specimens due to its thickest chromized layer on the surface. Comparing the anodic Tafel slopes of 1045-Ni-Cr(700-2) and 1045-Ni-CrC-Cr(700-2) at E_{corr}+10 mV, it shows that 1045-Ni-CrC-Cr(700-2) specimen was slight higher than 1045-Ni-Cr(700-2) specimen. Based on the polarization results, it was verified that the chromizing process could notably enhance the corrosion resistance of AISI 1045 steel and the addition of an electroplating Cr/C pretreatment step leading to the formation of a thicker Cr-rich layer improves the corrosion resistance. Based on our experimental observation, the specimen 1045-Ni-Cr(700-2) and 1045-Ni-CrC-Cr(700-2) had better corrosion resistance and these two specimens were selected for further study.
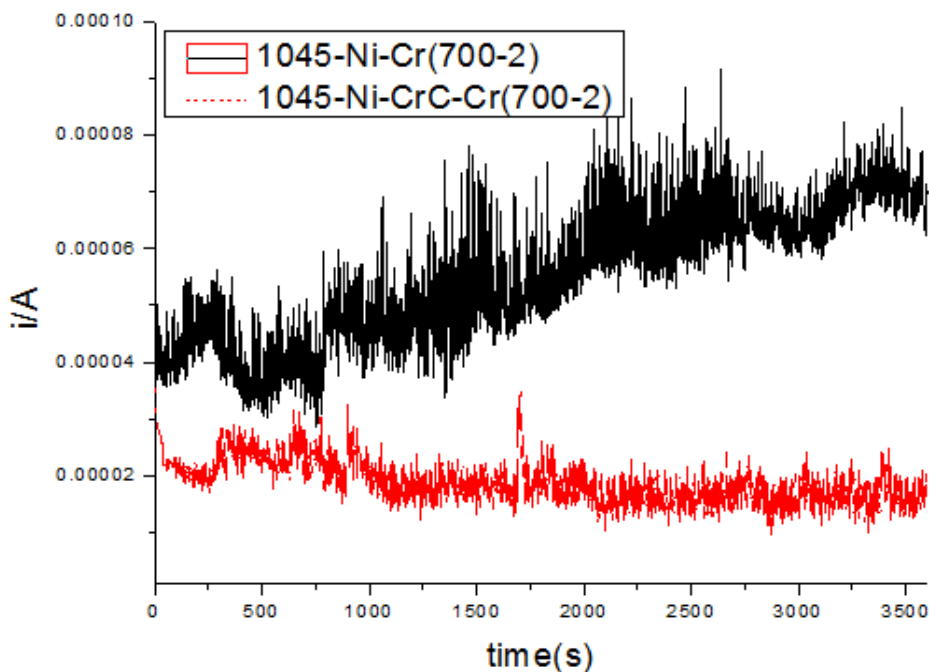

Figure 7. Potentiostatic curves of the 1045-Ni-Cr(700-2), and 1045-Ni-CrC-Cr(700-2) measured in simulated cathodic environment of PEMFC.

In order to evaluate the long-term corrosion resistance, the potentiostatic polarization test was also performed to examine the stability of 1045-Ni-CrC-Cr(700-2) and 1045-Ni-Cr(700-2) by monitoring the variation of current density as a function of time in a 0.5M H_2SO_4 solution at 80°C for a total time of 1 h. The potential of 0.6 V was loaded and air was purged to the working electrode to simulate the cathode environment of PEMFC. The current density of specimens as a function of time was plotted in Fig. 7. The current density of 1045-Ni-CrC-Cr(700-2) for 1 h exhibits a low stable value of 1.86 $\times 10^{-6}$ A cm^{-2} during the whole test, indicating that 1045-Ni-CrC-Cr(700-2) is stable under the cathode environment. However, the current density of 1045-Ni-Cr(700-2) increases gradually with time after the testing time of 500 S in the potentiostatic experiment, suggesting the 1045-Ni-Cr(700-2) at cathodic working environment of PEMFC is not as stable as that in potentiodynamic test environment. Comparing with the environment of potentiodynamic test, the environment in potentiostatic test (higher voltage and higher temperature) is harsher. Therefore, the specimen 1045-Ni-Cr(700-2) is susceptible in the simulated cathode environment of PEMFC. It indicates that the chromized AISI 1045 steel by Ni and Cr/C electroplating pretreatment exhibits better anticorrosion properties than that by Ni electroplating pretreatment. It could be due to the thicker chromized layer, which can effectively protect the steel from attack after long-term exposure in the simulated cathode environment of PEMFC.
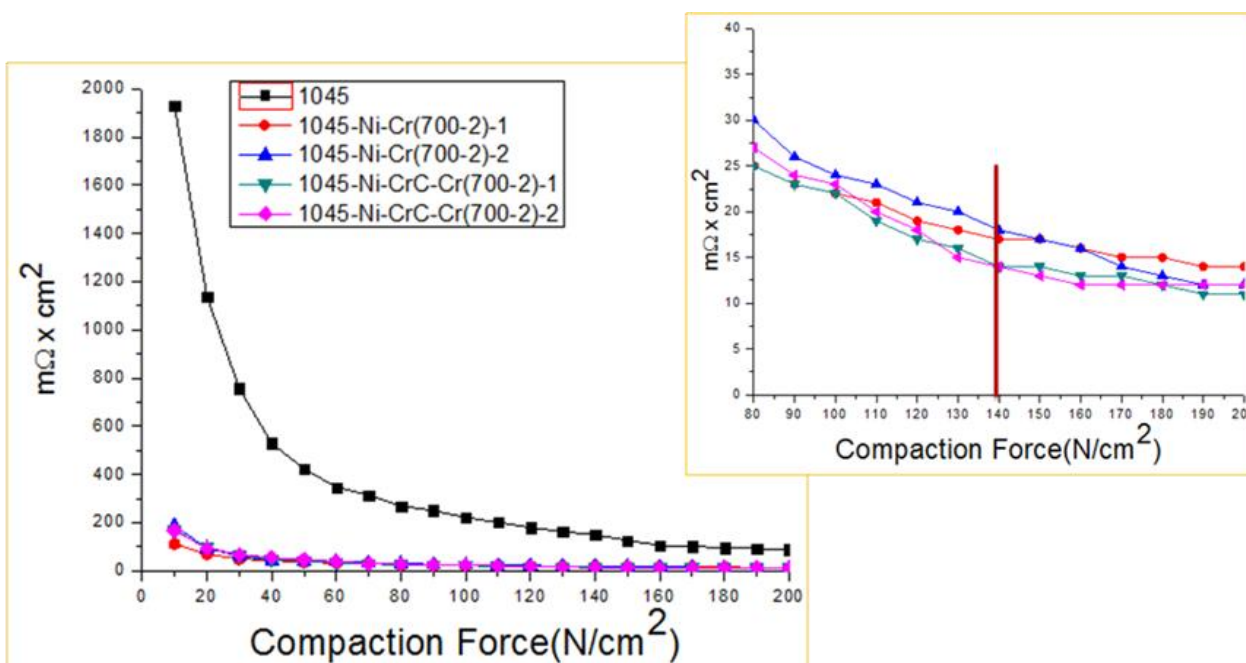
3.4 Interfacial contact resistance (ICR)

Figure 8. Interfacial contact resistances of bare 1045 steel and coated 1045 steel specimens as a function of compaction force.

The interfacial contact resistances of 1045-Ni-CrC-Cr(700-2) and 1045-Ni-Cr(700-2) specimens as measured at different compaction forces are shown in Fig. 8. For comparing the interfacial contact resistance of the chromized steels with commercial stainless steels, the value of

interfacial contact resistance for the untreated AISI 1045 steel, measured under the same conditions, is also shown in this figure. It is observed that the contact resistance is decreased with increasing compaction force. This is due to that the effective contact area is increased with increasing pressure. However, the contact resistance does not change almost at higher compaction force. This is related to the effective contact area is not increased further when the pressure is increased to a certain value. Many investigators have also obtained similar results [8,26,27]. The values of interfacial contact resistance for different specimens measured at a compaction pressure of 140 Ncm^{-2} are shown in Table 5.

Table 5. The interfacial contact resistances of bare and various coated steels under the compaction force of $140Ncm^{-2}$.

Code-name of specimen	$(m\Omega \times cm^2)$
1045	149
1045-Ni-Cr(700-2)-1	17
1045-Ni-Cr(700-2)-2	18
1045-Ni-CrC-Cr(700-2)-1	14
1045-Ni-CrC-Cr(700-2)-2	14

At the compaction force of 140 Ncm^{-2}, the interfacial contact resistance is approximately 17.5 and 14 $m\Omega$-cm^2 for specimen 1045-Ni-Cr(700-2) and 1045-Ni-CrC-Cr(700-2), respectively, and is much lower than 140 Ncm^{-2} for the untreated AISI 1045 steel under the same condition. Refer to previous studies [35-37], composition and roughness of the coating are the main factors to affect ICR. In general, the Fe-based steels with chromized coatings composed mainly of chromium carbides and chromium nitrides will possess higher conductivity than the bare steels with primarily chromium oxides on the surface [38]. Therefore, the lowest ICR value is expected for the specimen 1045-Ni-CrC-Cr(700-2) based on its high contents of chromium carbides and chromium nitrides within a dense and continuous chromized coating. Additionally, the contact resistance value of 1045-Ni-Cr(700-2) and 1045-Ni-CrC-Cr(700-2) specimens meets the U.S. DOE target for bipolar plate application (< 20 $m\Omega cm^2$ at 140 N cm^{-2}) [34].

3.5 Contact angle

It is well known that the water management is critical to achieve high performance and durability of PEMFC [39, 40]. When PEMFC is worked, water produced by the cathode reaction will accumulate at the flow field. If water could not be removed in time, it will block the channel through which the reactant Furthermore, the water adhering on the surface of bipolar plate accelerates the corrosion of metal bipolar plate. Therefore, the performance of fuel cell was directly affected by the hydrophilic and hydrophobic of the channel areas [41, 42]. It has been reported [43] that bipolar plate with high surface energy (hydrophobic) would be helpful for water removal in the stack and beneficial

to the water management. Contact angle measurement is a simple and direct method to characterize the hydrophilicity of sample surfaces. A surface can be considered as hydrophilic if the contact angle is <90˚ or hydrophobic if the angle is >90˚.
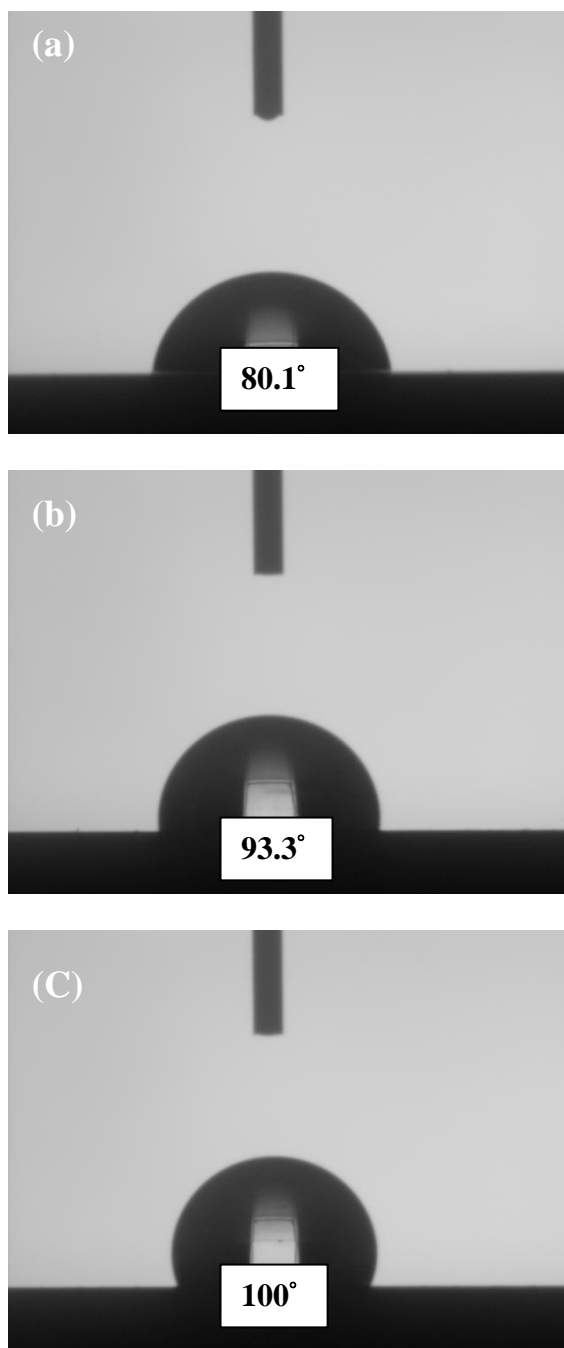

Figure 9. Contact angle of (a) bare 1045 carbon steel, (b) specimen 1045-Ni-Cr(700-2), (c) specimen 1045-Ni-CrC-Cr(700-2) with water.

The contact angles of the untreated AISI 1045 steel, 1045-Ni-Cr(700-2) and 1045-Ni-CrC-Cr(700-2) with water are shown in Fig. 9. It is observed that the contact angles of water on specimens 1045-Ni-CrC-Cr(700-2) and 1045-Ni-Cr(700-2) are 100˚ and 93.3˚, respectively, and the contact angle

of untreated AISI 1045 steel is only about 80.1˚. Obviously, both AISI 1045 steels coated with chromized layer have a bigger contact angle than that of untreated AISI 1045 steel. It indicates the untreated 1045 steel is the most hydrophilic among all tested specimens. This result might be attributed to the existence of corrosion product, Fe_2O_3, on the surface of untreated 1045 steel, leading to a better affinity with water than the chromium carbide on the surface of the chromized specimens. According to the contact angle measurements, it indicates that the chromized coatings can significantly enhance the hydrophobic property of 1045 steel due to the coatings comprised large amounts of hydrophobic chromium carbides and chromium nitrides.

4. CONCLUSIONS

In this work, a low cost AISI 1045 carbon steels with various pretreatments (i.e. electroplated Ni and Ni/CrC layer, respectively) before low temperature pack chromization, and its properties for application to PEMFCs were studied. The XRD results indicated that the composition both of 1045-Ni-Cr(700-2) and 1045-Ni-CrC-Cr(700-2) are composed of chromium carbides and chromium nitrides. The polarization results show that the 1045-Ni-CrC-Cr(700-2) specimen exhibits the lowest corrosion current density, 8.37×10^{-8} Acm^{-2}, in the potentiodynamic testing. Both interfacial contact resistances of 1045-Ni-Cr(700-2) and 1045-Ni-CrC-Cr(700-2) are lower than raw 1045 steel, and the 1045-Ni-CrC-Cr(700-2) possesses the lowest contact resistance value about 14 mΩ-cm^2. Furthermore, the 1045-Ni-CrC-Cr(700-2) presents the highest contact angle about 100˚. Based on the excellent properties present above, the pretreatments of electroplated Ni/CrC layers combined with low temperature pack chromization process can significantly improve the properties of carbon steel bipolar plate.

References

1. H. Wang, M.A. Sweikart, J.A. Turner, *J. Power Sources*, 115 (2003) 243-251.
2. H.Y. Jung, S.Y. Huang, P. Ganesan, B.N. Popov, *J Power Sources*, 2 (2009) 972-5.
3. J. Liu, F. Chen, Y.G. Chen, D.M. Zhang, *J Power Sources,* 187 (2009) 500-504.
4. R.A. Antunes, M.C.L. Oliveira, G. Ett, V. Ett, *Int. J. Hydrogen Energy*, *35*(2010), 3632-3647.
5. H. Tawfik, Y. Hung, D. Mahajan, *J. Power Sources,* 163 (2007) 755-767.
6. R.G. Reddy, V.Nikam, S.R. Collins, P.C. Williams, G.H. Schiroky, G.W. Henrich, *Electrochim. Acta*, 53 (2008) 2743-2750.
7. C.H. Lin, S.Y Tsai, *Applied Energy,* 100 (2012) 87-92.
8. C.Y. Bai, M.D. Ger, M.S. Wu, *Int. J. Hydrogen Energy*, 34 (2009) 6778-6789.
9. A. Hermann, T. Chaudhuri, P. Spagnol, *Int. J. Hydrogen Energy,* 30 (2005) 1297-1302.
10. M. Kumagai, S.T. Myung, S. Kuwata, R. Asaishi, H. Yashiro, *Electrochim. Acta*, 53 (2008) 4205-4212.
11. H. Wang, J.A. Turner, M.P. Brady, *ECS Transactions,* 11 (2007) 1461-1471.
12. Y. Fu, M. Hou, H. Xu, Z. Hou, P. Ming, Z. Shao, B. Yi, *J. Power Sources,* 182 (2008) 580-584.
13. M.S. Park, Y.M. Kang, J.H. Kima, G.X. Wang, S.X. Dou, H.K. Liu, *Carbon*, 46 (2008) 35-40.
14. S.H. Wang, J. Peng, W.B. Lui, J.S. Zhang, *J. Power Sources,* 162 (2006) 486-491.
15. W.S. Jeon, J.G. Kim, Y.J. Kim, J.G. Han, *Thin Solid Films,* 516 (2008) 3669-3672.
16. Y. Wang, D.O. Northwood, *J. Power Sources,* 165 (2007) 293-298.

17. W.Y. Ho, H.J. Pan, C.L. Chang, D.Y. Wang, J.J. Hwang, *Surf. Coat. Technol.,* 202 (2007) 1297-1301.
18. H. Sun, K. Cooke, G. Eitzinger, P. Hamilton, B. Pollet, *Thin Solid Films,* 528 (2013) 199-204.
19. S.T. Myung, M. Kumagai, R. Asaishi, Y.K. Sun, H. Yashiro, *Electrochem. Commun.,* 10 (2008) 480-484.
20. E.A. Cho, U.S. Jeon, S.A. Hong, I.H. Oh, S.G. Kang, *J. Power Sources,* 142 (2005) 177-183.
21. H. Wang, J.A. Turner, X. Li, G. Teeter, *J. Power Sources* 178 (2008) 238-247.
22. H. Wang, J.A. Turner, *J. Power Sources,* 170 (2007) 387-394.
23. C.Y. Wei, F.S. Chen, *Mater. Chem. Phys.,* 91 (2005) 192-199.
24. L. Levin, A. Ginzburge, L. Klinger, T. Werber, A. Katsman, P. Schaaf, *Surf. Coat. Technol.,* 106 (1998) 209–213.
25. Z.B. Wang, J. Lu, K. Lu., *Acta Mater.*, 53 (2005) 2081-2089.
26. C.Y. Bai, J.L. Lee, T.M. Wen, K.H. Hou, M.S. Wu, M.D. Ger, *Appl. Surf. Sci.,* 257 (2011) 3529-3537.
27. C.Y. Bai, T.M. Wen, K.H. Hou, M.D. Ger, *J. Power Sources*, 195(2010) 779-786.
28. J.W. Lee, and J.G. Duh, *Surf. Coat. Technol.* 177 (2004) 525-531.
29. C.Y. Bai, M.D. Ger, M.S. Wu, *Int. J. Hydrogen Energy* 34 (2009) 6778-6789.
30. Y. Nakagawa, Y. Tanji, H. Morita, H. Hiroyoshi, H. Fujimori, *J. Magnetism and Magnetic Materials*, 10 (1979) 145-151.
31. R.J. Tain, J.C. Sun, L. Wang, *J. Power Sources* 163 (2007) 719-724.
32. D.H. Han, W.H. Hang, H.S. Choi, J.J. Lee, *Int. J. Hydrogen Energy* 34 (2009) 2387-2395.
33. Y. Fu, M. Hou, G. Lin, J. Hou, Z. Shao, B. Yi, *J. Power Sources* 176 (2008) 282-286.
34. S. Karimi, N. Fraser, B. Roberts, F.R. Foulkes, *Adv. Mater. Sci. Eng*., 2012 (2012).
35. S.B. Lee, K.H. Cho, W.G. Lee, H. Jang, *J. Power Sources,* 187 (2009) 318-323.
36. B. Avasarala, P. Haldar, *J. Power Sources,* 188 (2009) 225.
37. H. Wang, M.P. Brady, G. Teeter, J.A. Turner, *J. Power Sources,* 138 (2004) 86-93.
38. C.Y. Bai, T.M. Wen, M.S Huang, K.H. Hou, M.D. Ger, S.J. Lee, *J. Power Sources,* 195 (2010) 5686-5691.
39. A.P. Sasmito, J.C. Kurnia, A.S. Mujumdar, *Energy*, 44 (2012) 278-291.
40. Z. Lu, C. Rath, G. Zhang, S.G. Kandlikar, *Int. J. Hydrogen Energy,* 36 (2011) 9864-9875.
41. M. Shoyama, T. Tomimura, S. Mizutani, *ECS Transactions*, 17(1) (2009) 461-464.
42. Fatma Gül Boyaci San, Isil Isik-Gulsac, *Int. J. Hydrogen Energy,* 38 (2013) 4089-4098.
43. Y. Fu, G Lin, M. Hou, B. Wu, Z. Shao, B. Yi, *Int. J. Hydrogen Energy,* 34 (2009) 405-409.